Published online 4 June 2008

Nucleic Acids Research, 2008, Vol. 36, No. 12 ***4079–4087***
doi:10.1093/nar/gkn351

Structural polymorphism of intramolecular quadruplex of human telomeric DNA: effect of cations, quadruplex-binding drugs and flanking sequences

Timur I. Gaynutdinov, Ronald D. Neumann and Igor G. Panyutin*

Department of Nuclear Medicine, Warren G. Magnuson Clinical Center, National Institutes of Health, Bethesda, MD 20892-1180, USA

Received March 27, 2008; Revised May 12, 2008; Accepted May 15, 2008

ABSTRACT

G-quadruplex structures formed in the telomeric DNA are thought to play a role in the telomere function. Drugs that stabilize the G-quadruplexes were shown to have anticancer effects. The structures formed by the basic telomeric quadruplex-forming unit $G_3(TTAG_3)_3$ were the subject of multiple studies. Here, we employ ^{125}I-radioprobing, a method based on analysis of the distribution of DNA breaks after decay of ^{125}I incorporated into one of the nucleotides, to determine the fold of the telomeric DNA in the presence of TMPyP4 and telomestatin, G-quadruplex-binding ligands and putative anticancer drugs. We show that d[$G_3(TTAG_3)_3$ ^{125}I-CT] adopts basket conformation in the presence of NaCl and that addition of either of the drugs does not change this conformation of the quadruplex. In KCl, the d[$G_3(TTAG_3)_3$^{125}I-CT] is most likely present as a mixture of two or more conformations, but addition of the drugs stabilize the basket conformation. We also show that d[$G_3(TTAG_3)_3$^{125}I-CT] with a 5′-flanking sequence folds into (3+1) type 2 conformation in KCl, while in NaCl it adopts a novel (3+1) basket conformation with a diagonal central loop. The results demonstrate the structural flexibility of the human telomeric DNA; and show how cations, quadruplex-binding drugs and flanking sequences can affect the conformation of the telomeric quadruplex.

INTRODUCTION

Human telomeres are capped with several thousands of d(GGGTTA)·d(CCCAAT) repeats with 8–150 d(GGGTTA) repeats in the single-stranded 3′ overhang (1,2). Single-stranded oligonucleotides containing runs of Gs have been shown to form intra- and inter-molecular structures stabilized by three or more G-quartets forming a G-quadruplex (3–7). Shelterin, a specialized protein complex that protects the ends of the chromosomes has been identified and characterized (8). One of these proteins POT1 specifically binds to the 3′ telomeric overhangs, presumably preventing them from forming the quadruplex structures (9,10). The quadruplex structures can inhibit the activity of telomerase, an RNA template containing enzyme that adds the telomeric repeats to the ends on the chromosomes (9). The telomerase activity is essential for proliferation of cancer cells; and, therefore, inhibition of the telomerase could stop tumor growth (11). Several drugs that specifically bind to G-quadruplexes were shown to have anticancer activity (12); the most studied of them is a porphyrin TMPyP4 (13) and telomestatin (14).

For the rational design of the G-quadruplex-binding drugs, it is important to know the molecular structure of the human telomeric quadruplex. Several such structures were recently solved by both NMR and X-ray crystallography (15). Depending upon the flanking sequences and ionic conditions the human telomeric oligonucleotides in solution were shown to fold into an antiparallel basket conformation with alternating directions of the G_3 runs (16), and so-called (3 + 1) mixed conformation with three parallel and one antiparallel orientation the G_3 runs (17–19) (Figure 1). In the basket conformation, all the loops are lateral, i.e. they run across the top or the bottom G-quartet with two on the top (Figure 1) connecting neighboring G-sides while one at the bottom running diagonally. The (3 + 1) conformation contains two lateral loops and one double-chain-reversal loop that runs across the stack of G-quartets. Two conformers of the (3 + 1) conformation were identified, type 1 and 2, with either first (type 1) or the last (type 2) loop being the double-chain-reversal one (20–23). In the crystal, all-parallel propeller conformation of the quadruplex

*To whom correspondence should be addressed. Tel: +1 301 496 8308; Fax: +1 301 480 9712; Email: igorp@helix.nih.gov

was found with all the loops being double-chain-reversal (24). In addition, telomeric oligonucleotides can fold into another antiparallel conformation, so-called 'chair' that has a lateral loop at the bottom of the G-quadruplex (19,25), although the 3D structure of the chair conformation has not been solved yet either by X-ray or by NMR.

Structural methods like X-ray crystallography and NMR are indispensable in obtaining the detailed 3D conformation of the different folds of G-quadruplex. However, given the highly polymorphic nature of the telomeric DNA, important information on the transitions between the folds, kinetics, small molecule binding etc. was obtained by various biochemical methods (26–35). We applied ^{125}I-radioprobing to study the fold of telomeric oligonucleotides. This method is based on the measurement of the probability of strand breaks produced by decay of ^{125}I placed into one of the nucleotide (36). The probability of DNA breaks caused by decay of ^{125}I is inversely related to the distance between the radionucleotide and the sugar unit of the DNA backbone where the break occurs; hence, the conformation of a DNA backbone can be obtained from the distribution of breaks (37). In our previous study (25), we placed ^{125}I-dC instead of T into one of the TTA loops of the telomeric oligonucleotides, and showed the presence in solution of two antiparallel conformations of human telomeric quadruplex, basket and chair. However, placement of the radioiodine into the flexible loop introduced some uncertainty to its location diminishing the resolution with which the structural information could be obtained.

Herein, we extend our radioprobing studies of the telomeric quadruplex structures by placing ^{125}I-dC immediately next to the 3′-end of the telomeric repeats (Figure 1). Using this approach, we show that a telomeric oligonucleotide consisting of four G_3 runs, three TTA

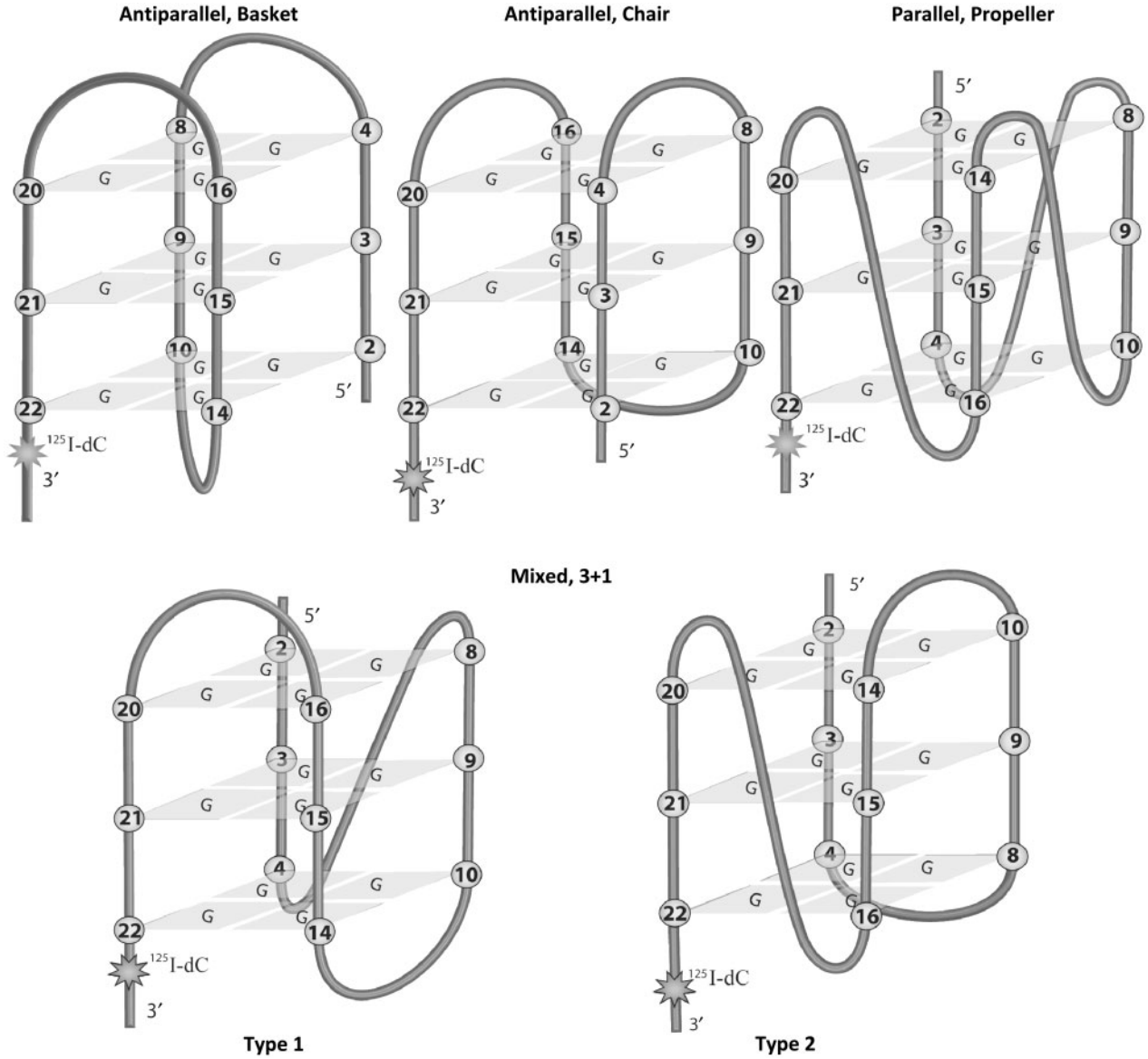

Figure 1. Schematic diagram of possible intramolecular conformations of human telomeric quadruplexes.

loops and ^{125}I-dC and T at the 3′-end folds into a basket conformation in the presence of NaCl, in agreement with earlier NMR results (16). In KCl, such a 'minimal' G-quadruplex forming telomeric oligonucleotide most likely exist as a mixture of two or more conformations. Importantly, for the first time we show that in the presence of G-quadruplex-binding drugs TMPyP4 and telomestatin this oligonucleotide forms the basket conformation both in NaCl and in KCl. We also studied the effect of the 5′-flanking sequence addition to this oligonucleotide on the fold of G-quadruplex, and propose a new conformation of the (3 + 1) fold with a diagonal loop at the bottom of the structure.

MATERIALS AND METHODS

Oligodeoxyribonucleotides and reagents

All oligodeoxyribonucleotides (ODNs, Table 1) were synthesized on an ABI394 DNA synthesizer (PE Applied Biosystems, Foster City, CA, USA), and purified by denaturating polyacrylamide gel electrophoresis (PAGE) as described in detail in ref. (25). The concentration of single-stranded ODN was measured at 260 nm on a HP 8452A Diode Array Spectrophotometer, and was calculated with the extinction coefficient calculator software (http://www.basic.northwestern.edu/biotools/oligocalc.html).
Cationic porphyrin 5,10,15,20-tetra(*N*-methyl-4-pyridyl)-porphin (TMPyP4) was purchased from Calbiochem (La Jolla, CA, USA); telomestatin was kindly provided by Dr Kazuo Shin-ya (AIST, Tokyo, Japan)

Labeling and purification of ODNs

The telomeric ODNs were labeled with ^{125}I using [^{125}I]-IdCTP and Klenow fragment of DNA polymerase I by primer extension reaction (38). The detailed protocol for ^{125}I labeling was as follows: 2 µl of 10× Klenow fragment of DNA polymerase I buffer [500 mM Tris–HCl (pH 8.0), 50 mM $MgCl_2$ and 10 mM DTT], 1 µl of 10 µM duplexes (pairs primer and template—**III** and **IV**; **VI** and **VII** (Table 1) were annealed in equimolar amounts) and 16 µl of H_2O were added to freshly dried 120 µCi [^{125}I]-IdCTP. After 15 min at RT, 1 µl of 10 U/µl Klenow fragment of DNA polymerase I (Fermentas, Hanover, MD, USA) was added. After 15 min, 2 µl of 100 mM dNTP was added and after additional 15 min incubation, the reactions were stopped with 1.5 µl of 0.5 M EDTA. The reaction mixtures were purified by MicroSpin G-25 columns (Amersham Pharmacia Biotech, Piscataway, NJ, USA) to remove free [^{125}I]-IdCTP. The labeled ODNs were separated and further purified from the template by purification with denaturing PAGE. The ODNs were ^{32}P 5′-end labeled using T4 Polynucleotide Kinase (Fermentas) following the standard protocol.

Preparation of G-4 quadruplexes

The telomeric ODNs were incubated in presence or absence of the TMPyP4 or telomestatin in radioprobing buffer (RB) solution [20 mM Tris–HCl (pH 7.4), 10% DMSO and 1 mM EDTA] with addition of 100 mM NaCl or 100 mM KCl at 37°C for 1 h. Than samples were quickly frozen in liquid nitrogen and stored at −80°C for 2 weeks to accumulate ^{125}I-induced DNA strand breaks.

DNA strand break analysis

After 2 weeks, the samples were thawed and the strand breaks were analyzed by 12% denaturing PAGE. The DNA strand breaks were quantified using a BAS-2500 Bioimager (FUJI Medical Systems USA, Stamford, CT, USA). To measure the intensity of the individual bands, the intensity profile of each lane was generated from the digitized gel image using SAFA software (39). The probability of breaks were calculated from the areas of the individual peaks using a recursive formula and assuming that probability of breaks at [^{125}I]-IdC equals 1 as described in detail in ref. (36). Briefly, if there is >1 break/decay then only the break closest to the ^{32}P-labeled 5′-end of the oligonucleotide will be detected. To obtain the probabilities of breaks in *i*-th position (p_i) we used the recursive expression: $p_i = F_i/(1 - p_{i-1})(1 - p_{i-2}).(1 - p_1)$, where is F_i is the observed frequency of breaks at nucleotide in position *i*.

RESULTS

Radioprobing rationale

In our previous study, we placed the ^{125}I-dC residue into one of the loops of the telomeric quadruplex in order to have the radioiodine inside the structure (25). This approach has certain limitations due to the flexibility of the loops resulting in an uncertainty in the position of radioiodine (25). In this study, we placed ^{125}I-dC next to the last G at the 3′-end of the telomeric quadruplex (Table 1) in an attempt to reduce the uncertainty in the ^{125}I position. Having radioiodine in the 'corner' of the G-quadruplex also simplifies the analysis of the data on distribution of ^{125}I-induced breaks.

Table 1. Oligonucleotides used in this study

I	5′-^{32}P-$G_2G_3G_4T_5T_6A_7G_8G_9G_{10}T_{11}T_{12}A_{13}G_{14}G_{15}G_{16}T_{17}T_{18}A_{19}G_{20}G_{21}G_{22}C^*_{23}T_{24}$	
	Oligonucleotides used for ^{125}I-labeling of **I**	
III	5′-GGGTTAGGGTTAGGGTTAGGG	Primer
IV	3′-BTTTTTTCCCAATCCCAATCCCAATCCCGA	Complementary template
V	5′-^{32}P-$G_{-8}T_{-7}G_{-6}C_{-5}A_{-4}G_{-3}T_{-2}A_{-1}G_1G_2G_3G_4T_5T_6A_7G_8G_9G_{10}T_{11}T_{12}A_{13}G_{14}G_{15}G_{16}T_{17}C_{18}A_{19}G_{20}G_{21}G_{22}C^*_{23}T_{24}$	
	Oligonucleotides used for ^{125}I-labeling of **V**	
VI	5′-GTGCAGTAGGGGTTAGGGTTAGGGTCAGGG	Primer
VII	3′-BTGTGTGTACACGTCATCCCCAATCCCAATCCCAGTCCCGA	Complementary template

B, biotin; C*, [^{125}I]-dC.

Figure 2A shows average distances from the C1′ of the G22 to the sugars of the guanines in the core for three different conformations of the G-quadruplex calculated as described previously (25). The plots reflect different folds of DNA chain in the quadruplex conformations. In all conformations, the distances sharply increase as we move from G22 to G20 along the DNA chain. In the basket and (3 + 1) type 1 conformations, the distances decrease from G16 to G14; on the contrary, these distances increase in the propeller fold reflecting a different conformation of the A19-T17 loop. In the propeller and (3 + 1) type 1 conformations, the G10-G8 side of G-quadruplex is the most distant from the 3′ corner, while in the basket fold the G4-G2 side is the most distant. In general, the distances increase as we move from the G22 position in the bottom of the core (as it is oriented in Figure 1); and they are the longest to the nucleotides located in the side that is diagonally across the G-quadruplex from G22, as it could be intuitively expected from the sketches presented in Figure 1. If '↑' indicates the increase in distances and '↓' the decrease, then the basket conformation can be described as G22↑G20, G16↓G14, G10↑G8, G4↓G2, '3 + 1' type 1 as G22↑G20, G16↓G14, G10↑G8, G4↑G2, and propeller as G22↑G20, G16↑G14, G10↑G8, G4↑G2.

At the same time, if the distances are re-plotted according to the positions of the guanines in the core structure, numbered in the same order as in the propeller conformation, (as opposed to the numbering according to their position along the DNA chain as in Figure 2A), the graphs became very similar (Figure 2B). This shows that all three G-quadruplexes are similar in terms of the distances from the 3′-corner of the core to the sugars of the guanines. Therefore, differences in the breaks distribution produced by decay of ^{125}I located in the 3′-corner of the G-quadruplex should truly reflect the different folds of the chain of the telomeric DNA.

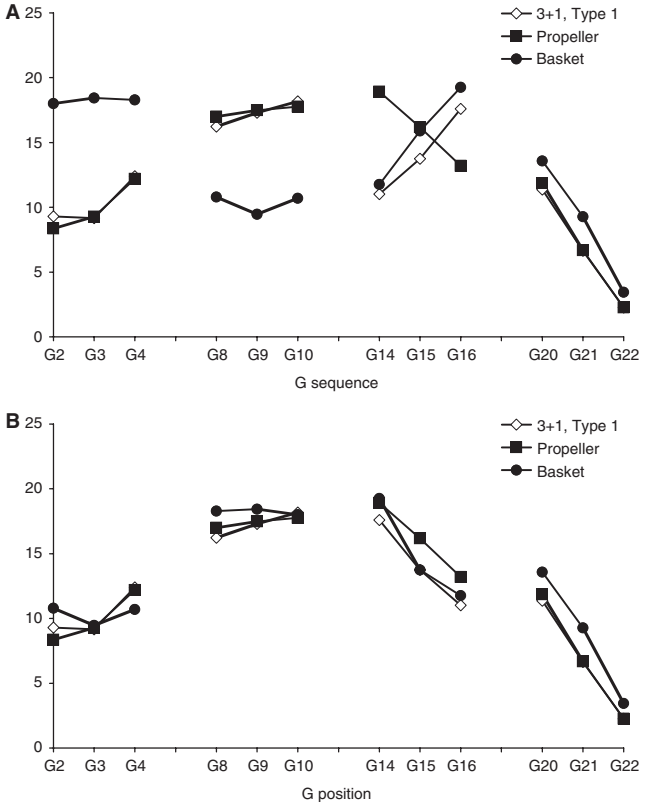

Figure 2. Average distances (in angstroms) from the C1′ of the G22 to the sugars of the guanines in the core for three different conformations of the G-quadruplex; open diamonds—(3 + 1) type 1, PDB ID 2GKU (18); black squares—propeller, PDB ID 1KF1 (24); black circles—basket PDB ID 143D (16). (**A**) Guanines numbered according to their position along the DNA chain; (**B**) average distances re-plotted according to the positions of the guanines in the core and numbered in the same order as in the propeller conformation.

Conformation of I in Na^+

Figure 3 illustrates our radioprobing approach to determine intramolecular fold of oligonucleotide **I**, d[$G_3(TTAG_3)_3$^{125}I-CT]. Panel A shows the analysis of DNA breaks in denaturing PAGE. Panel B represents the measurement of the intensity of the breaks by densitometry and peak deconvolution (for details see the Materials and methods section). The resulting probabilities of breaks at the individual nucleotides are plotted in panel C. The higher the probability of breaks the closer the nucleotide to the ^{125}I-dC at the 3′-end of the structure. Accordingly, the probability increases sharply from G20 to G22. The drop of the breaks probability from G14 to G16 shows that the former is closer to the bottom of the structure than the later. Likewise, the G10 is closer than G8. The graph in Figure 3C and the sketch in Figure 3D are oriented such that the arrows showing the increase in breaks probability correspond to the orientation of the GGG repeats in the G-quadruplex. Therefore, the structure can be described in terms of the orientation of the sides as G22↑G20, G16↓G14, G10↑G8 and G4↓G2. The G4 and G3 have the lowest probability of breaks. Hence, the nucleotides G4-G2 are located diagonally across from the ^{125}I-dC. This arrangement of the sides corresponds to the basket conformation of the quadruplex. Indeed, in other antiparallel fold, the chair conformation, the G10-G8 side would be the most distant from ^{125}I-dC and have the lowest breaks probability (Figure 1). Therefore, the predominant fold of **I** in NaCl solution is the basket conformation.

Conformation of I in K^+

Figure 4 shows the results of radioprobing experiment of oligonucleotide **I** in the presence of KCl. In contrast to the NaCl data, there is no clear increase or decrease in the breaks probability along G10-G8 and G16-G14 sides. In fact, it is impossible to say which side was the most distant from the ^{125}I-dC. Overall, the observed distribution of the probability of breaks does not correspond to any of the known folds of the G-quadruplex and most likely indicates that two or more conformations of **I** coexist in equilibrium in the presence of KCl.

Conformation of I with telomestatin

Figure 5 shows radioprobing of **I** in the presence of the G-quadruplex-binding drug telomestatin (14). The distributions of breaks have similar patterns in the presence

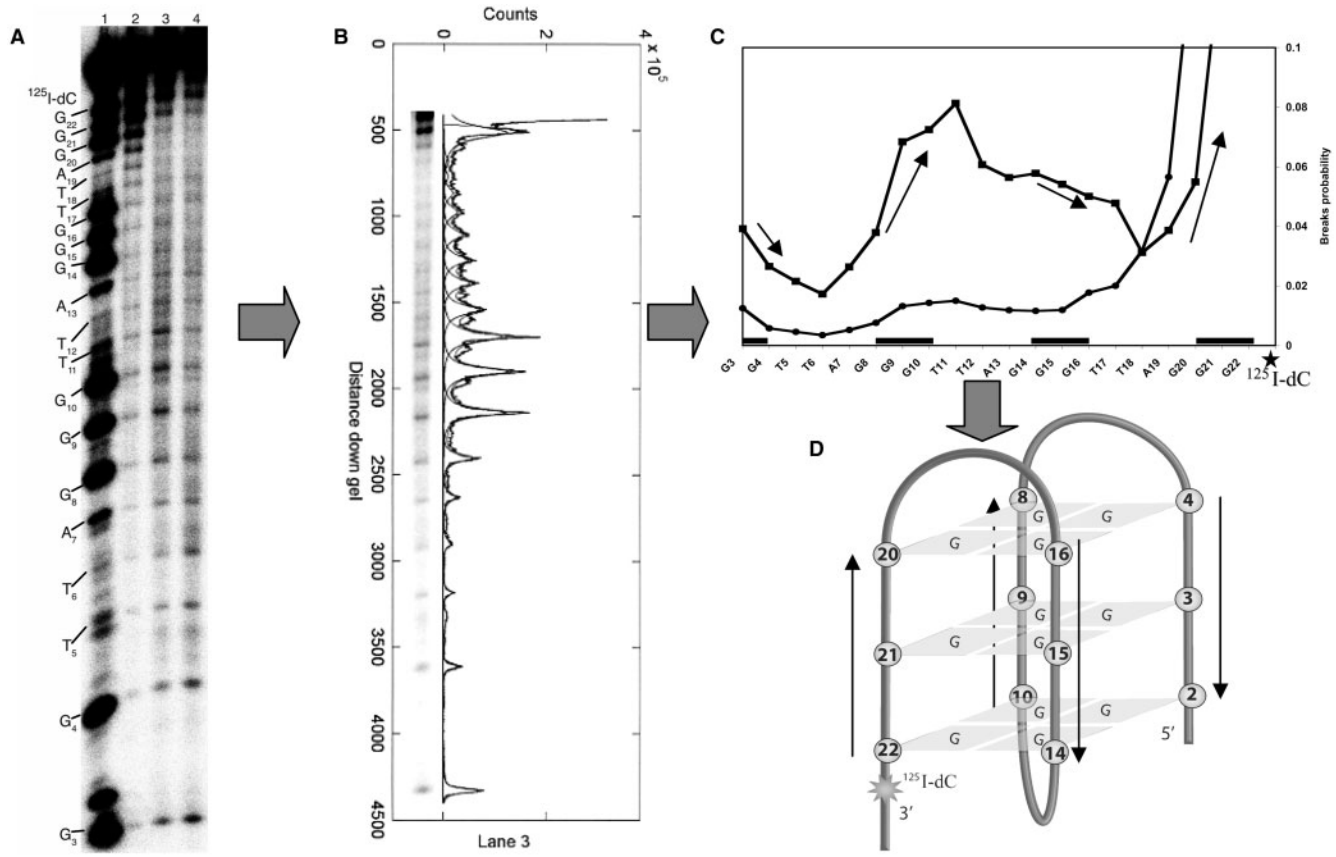

Figure 3. (**A**) Analysis of DNA breaks in telomeric oligonucleotide **I** by 12% denaturing PAGE. Lanes: 1–G sequencing ladder; 2–Duplex of **I** with complementary strand **IV**; 3–ODN **I** folded in RB + 100 mM NaCl; 4–ODN **I** folded in RB + 100 mM KCl; (**B**) analysis of break distribution in telomeric oligonucleotide **I** folded in the presence of 100 mM NaCl using SAFA software (39); (**C**) distribution of ^{125}I-induced strand break probability in telomeric oligonucleotide **I**. The samples were incubated (1 h at 37°C) in RB with addition of 100 mM NaCl (black squares) or in duplex with complimentary template **IV** (black circles). Arrows indicate increasing or decreasing probability of breaks along the G_3 runs. (**D**) Suggested conformation of ODN **I** in the presence of 100 mM NaCl, based on analysis of distribution of breaks probability. Arrows indicate increasing or decreasing distance from the position of ^{125}I along the G_3 runs.

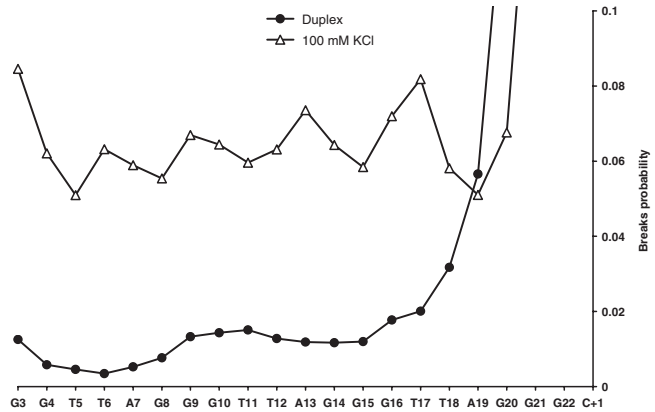

Figure 4. Distribution of ^{125}I-induced strand breaks probability in the telomeric oligonucleotide **I**. The samples were incubated for 1 h at 37°C in RB with addition of 100 mM KCl (open triangles); duplex with complimentary template **IV** (black circles).

of both NaCl and KCl and closely resemble the breaks distribution obtained in NaCl alone (Figure 3), i.e. G22↑G20, G16↓G14, G10↑G8, G4↓G2. As we rationalized above, such distribution with alternating directions of the G-sides and G4-G2 being the most distant from the ^{125}I-dC corresponds to the basket conformation of the G-quadruplex. Interestingly, the absolute values of the breaks probability are higher in KCl than in NaCl, reflecting, most likely, a more compact conformation of the basket quadruplex in KCl as compared to NaCl.

Conformation of I with TMPyP4

The distributions of breaks produced by decay of ^{125}I in **I** in the complex with cationic porphyrin TMPyP4 are shown in Figure 6. In the presence of both NaCl and KCl, the break distributions are consistent with the basket conformation of the quadruplex. The overall shape of the break distribution is slightly different from that observed in the complex with telomestatin (Figure 5) most likely reflecting different conformations of the loops. As with telomestatin, the quadruplex conformation in the presence of KCl is more compact than in NaCl judging by the higher absolute values of the breaks probability in KCl.

Effect of flanking sequences

Our data on the conformation of the human telomeric quadruplex in the presence of KCl presented above differ

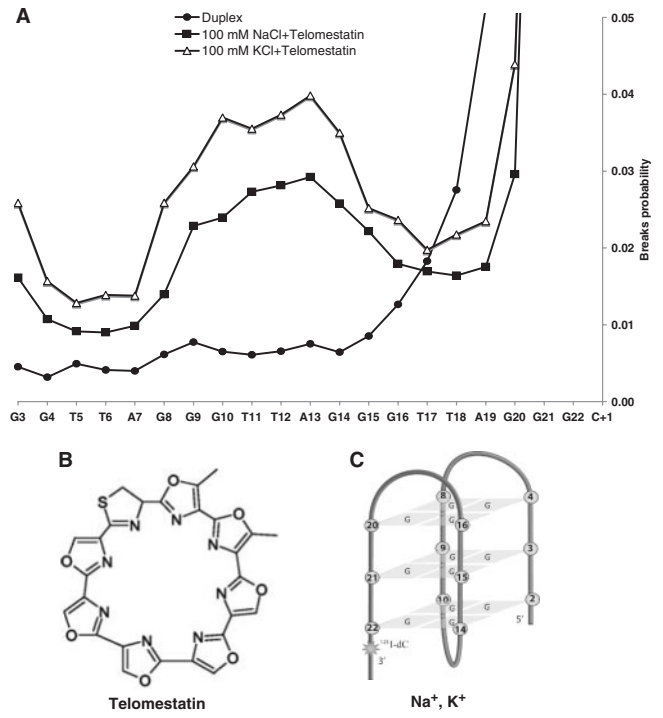

Figure 5. Distribution of ^{125}I-induced strand break probability in telomeric oligonucleotide **I**. The samples were incubated for 1 h at 37°C in RB with addition of 100 mM NaCl and 10 μM telomestatin (black squares); with addition of 100 mM KCl and 10 μM telomestatin (open triangles) or in duplex with complimentary template **IV** (black circles). The schemas show the chemical structure of telomestatin and the basket conformation of oligonucleotide **I**.

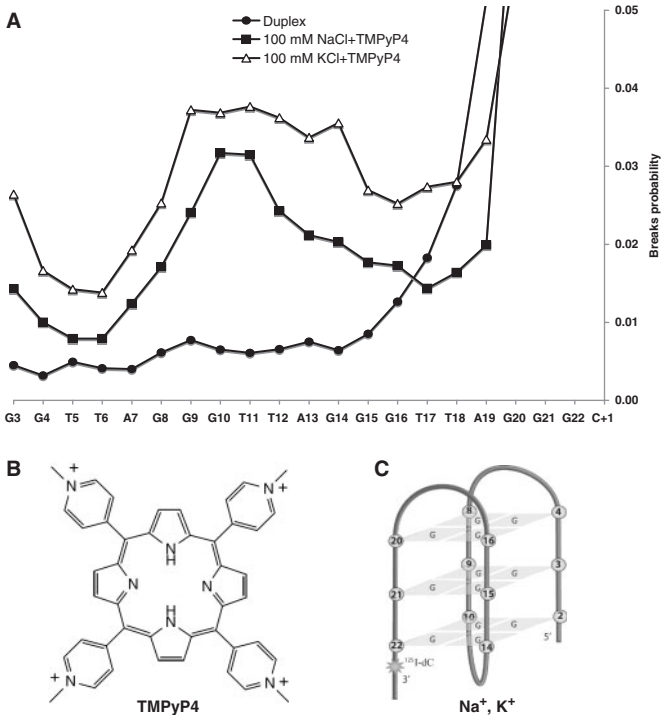

Figure 6. Distribution of ^{125}I-induced strand break probability in the telomeric oligonucleotide **I**. The samples were incubated in RB with addition of 100 mM NaCl and 10 μM TMPyP4 (closed squares); with addition of 100 mM KCl and 10 μM TMPyP4 (open triangles) or in duplex with complimentary template **IV** (closed circles). The schemas show the chemical structure of TMPyP4 and the basket conformation of oligonucleotide **I**.

from our previous radioprobing results. The main difference of this study is the use of oligonucleotide **I** that has no extra nucleotides on the 5′-end of the four telomeric repeats or so-called a 5′ tail. To test the effect of such a tail, we carried out radioprobing experiments with oligonucleotide **V** (Table 1). In fact, **V** has the same sequence of the 5′ tail that the oligonucleotide we used in our previous study (25), but the 3′ tail is now shorten to just two nucleotides, i.e. ^{125}IdC and T. The results of radioprobing of **V** are shown in Figure 7. The distributions of breaks are quite different in the presence of NaCl and KCl. The latter could be described in our terms as G22↑G20,G16↑G14,G10↓G8, G4↑G2 with the side G10-G8 being the most distant from the ^{125}IdC. This arrangement of the sides corresponds to the (3 + 1) structure of type 2 (Figure 7C). The quadruplex conformation of **V** in NaCl is G22↑G20,G16↓G14,G10↑ G8,G4↑G2. This arrangement of the sides could correspond to the (3 + 1) structure of type 1, but in this structure, the G10-G8 side would be the most distant from the ^{125}IdC (Figure 1). However, the results in Figure 7A show that the most distant side is the G4-G2 side. The structure that corresponds to such an arrangement of the sides is shown in Figure 7B. Additional evidence in favor of such conformation comes from the consideration of the breaks pattern in the loops. The break probabilities in NaCl show that the loop T11-A13 is the closest to ^{125}I-dC with T11 and A13 being equidistant, which is consistent with the structure shown in Figure 7B. This structure has a diagonal loop similar to the basket conformation of quadruplex (Figure 1), therefore we called it (3 + 1) basket structure.

DISCUSSION

We applied radioprobing to determine conformation of human telomeric DNA oligonucleotides by placing the ^{125}I labeled dC immediately next to the 3'terminal G_3 run of the basic telomeric quadruplex-forming unit $G_3(TTAG_3)_3$. An ideal location for the ^{125}I would be a defined site within one of the G-quartets forming the core of the quadruplex structure. Then, by measuring the break probabilities and comparing them with those, for example, in a duplex with known structure, it would be possible to obtain actual distances from the ^{125}I to the sugar backbone of the other nucleotides in the quadruplex, thus determining its conformation more precisely. Unfortunately, an effective procedure for iodination of guanine has not been developed so far; therefore, ^{125}I-dC remains the only choice for incorporation of radioiodine into DNA.

The position of ^{125}I-dC at the 3′ of the telomeric quadruplex is not exactly defined. Therefore, it was important to test our approach on a known conformation of the quadruplex. The first structure of human telomeric DNA was solved by NMR in 1993 in the presence of NaCl (16). It was shown that in these conditions d[$AG_3(TTAG_3)_3$] folded into a basket-type intramolecular quadruplex. Later, other quadruplex-forming sequences were shown

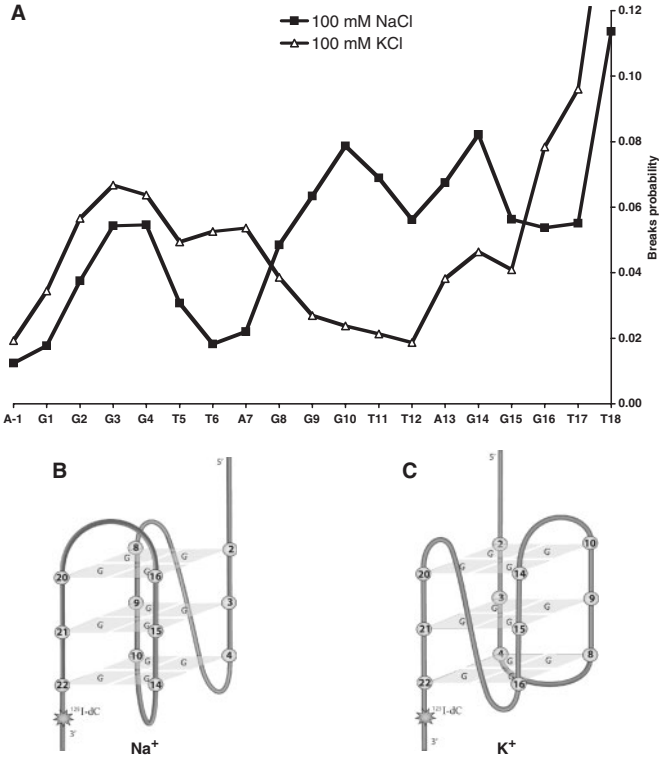

Figure 7. Distribution of ^{125}I-induced strand break probability in telomeric oligonucleotide **V**. The samples were incubated in radioprobing buffer with addition of 100 mM NaCl (black squares) or with addition of 100 mM KCl (open triangles). The schemas show suggested conformations of ODN **V** in the presence of NaCl and KCl, based on the analysis of distribution of breaks probability.

to adopt the basket conformation in the presence of NaCl (40). Our radioprobing data (Figure 3) confirmed folding of **I** into the basket conformation in NaCl. This result provided additional evidence for reliability of our approach.

The results of radioprobing of **I** in KCl were consistent with co-existence of two or more conformations. Authors of recent NMR studies arrived to a similar conclusion (17). They found that in KCl solutions nucleotides flanking the quadruplex-forming sequence are required to stabilize a single conformation. More recently, it was shown that by altering the nucleotides flanking $G_3(TTAG_3)_3$ basic telomeric quadruplex-forming unit one could stabilize type 1 or type 2 isoform of the (3 + 1) fold (22,23). In our oligonucleotide **I**, the quadruplex-forming unit has only two additional nucleotides, ^{125}I-dC and T that are unlikely to form the capping structures that stabilized different isomers of the (3 + 1) fold as it was observed in the NMR studies. It also worth noting that radioprobing, like NMR, allows obtaining reliable structural information when molecules in solution adopt a single or predominant conformation. Results obtained from a mixture of conformations are difficult to interpret, especially in the cases when the position of ^{125}I is not precisely determined (25).

Our data show that binding of the quadruplex-specific drugs, TMPyP4 and telomestatin, in both NaCl and KCl solutions, stabilized the basket conformation of **I**. For telomestatin, these results are in agreement with that obtained earlier based on CD spectra of the drug binding to the telomeric oligonucleotide (41). On the other hand, in co-crystals of a telomeric oligonucleotide and TMPyP4, the porphyrin was bound by stacking to the TTA loops of the quadruplex in the all-parallel propeller conformation (42). However, the close packing environment may have affected the quadruplex structure and the mode of the drug binding in the crystal. Other studies have proposed the possibility of the intercalating mode of binding of TMPyP4 to quadruplex, in particular in the presence of NaCl (43–45). As we noted earlier, our radioprobing data indicate that the guanines in quadruplex are more distant from ^{125}I-dC in NaCl than in KCl. Unfortunately, due to an uncertainty in the position of ^{125}I in our experiments we could not estimate absolute distances between the guanines in the neighboring G-quartets. Therefore, at this point, we can only speculate on the possibility of the intercalating mode of TMPyP binding in NaCl. Overall, our results suggest that there could be more than one mode of the TMPyP4 binding to the telomeric quadruplex.

Extension of **I** with additional nine nucleotides upstream of the telomeric repeats changed the fold of the quadruplex. The breaks distribution in oligonucleotide **V** is consistent with the (3 + 1) type 2 fold in KCl in agreement with NMR data on the telomeric oligonucleotides containing both 5′ and 3′ extensions (22,23). In NaCl, our radioprobing data predict a new conformation of telomeric quadruplex that we called (3 + 1) basket type. This conformation is different from (3 + 1) forms type 1 and type 2 by having a diagonal loop (Figure 7B). Thus, it appears that Na+ cations favor diagonal loops, although the structural reasons for this are not clear at this point. In our previous radioprobing experiments (25), we determined the chair quadruplex conformation of the telomeric oligonucleotide with 5′ and 3′ complementary extensions. We believe now that the formation of the duplex between the 5′ and 3′-flanking sequences could have affected the fold of the quadruplex favoring the chair conformation.

In summary, our results demonstrate that human telomeric quadruplex can adopt multiple conformations. The fold of the quadruplex depends on the presence and the makeup of 5′- and 3′-flanking sequences, the type of metal cations in solution as well as binding of quadruplex-specific drugs. To address questions about possible biological role of such structural plasticity of the telomeric quadruplex and the structure of the telomeric repeats inside living cells more realistic models of telomeric DNA, including multiple duplex telomeric repeats with single-stranded overhangs, need to be developed and studied. Radioprobing is one of the methods that perfectly fit for such studies, because it can be adapted to large DNA–protein assembles and even for *in situ* experiments.

ACKNOWLEDGEMENTS

We are grateful to Dr Kazuo Shin-ya for his generous gift of telomestatin. This research was supported by the Intramural Research Program of the NIH, Clinical Center. Funding to pay the Open Access publication

charges for this article was provided by Intramural Research Program of the NIH, Clinical Center.

Conflict of interest statement. None declared.

REFERENCES

1. Moyzis,R.K., Buckingham,J.M., Cram,L.S., Dani,M., Deaven,L.L., Jones,M.D., Meyne,J., Ratliff,R.L. and Wu,J.R. (1988) A highly conserved repetitive DNA sequence, (TTAGGG)n, present at the telomeres of human chromosomes. *Proc. Natl Acad. Sci. USA*, **85**, 6622–6626.
2. Sfeir,A.J., Chai,W., Shay,J.W. and Wright,W.E. (2005) Telomere-end processing the terminal nucleotides of human chromosomes. *Mol. Cell*, **18**, 131–138.
3. Gellert,M., Lipsett,M.N. and Davies,D.R. (1962) Helix formation by guanylic acid. *Proc. Natl Acad. Sci. USA*, **48**, 2013–2018.
4. Sen,D. and Gilbert,W. (1988) Formation of parallel four-stranded complexes by guanine-rich motifs in DNA and its implications for meiosis. *Nature*, **334**, 364–366.
5. Williamson,J.R., Raghuraman,M.K. and Cech,T.R. (1989) Monovalent cation-induced structure of telomeric DNA: the G-quartet model. *Cell*, **59**, 871–880.
6. Sundquist,W.I. and Klug,A. (1989) Telomeric DNA dimerizes by formation of guanine tetrads between hairpin loops. *Nature*, **342**, 825–829.
7. Panyutin,I.G., Kovalsky,O.I., Budowsky,E.I., Dickerson,R.E., Rikhirev,M.E. and Lipanov,A.A. (1990) G-DNA: a twice-folded DNA structure adopted by single-stranded oligo(dG) and its implications for telomeres. *Proc. Natl Acad. Sci. USA*, **87**, 867–870.
8. de Lange,T. (2005) Shelterin: the protein complex that shapes and safeguards human telomeres. *Genes Dev.*, **19**, 2100–2110.
9. Zaug,A.J., Podell,E.R. and Cech,T.R. (2005) Human POT1 disrupts telomeric G-quadruplexes allowing telomerase extension in vitro. *Proc. Natl Acad. Sci. USA*, **102**, 10864–10869.
10. Lei,M., Podell,E.R. and Cech,T.R. (2004) Structure of human POT1 bound to telomeric single-stranded DNA provides a model for chromosome end-protection. *Nat. Struct. Mol. Biol.*, **11**, 1223–1229.
11. Sun,D., Thompson,B., Cathers,B.E., Salazar,M., Kerwin,S.M., Trent,J.O., Jenkins,T.C., Neidle,S. and Hurley,L.H. (1997) Inhibition of human telomerase by a G-quadruplex-interactive compound. *J. Med. Chem.*, **40**, 2113–2116.
12. Cuesta,J., Read,M.A. and Neidle,S. (2003) The design of G-quadruplex ligands as telomerase inhibitors. *Mini Rev. Med. Chem.*, **3**, 11–21.
13. Izbicka,E., Wheelhouse,R.T., Raymond,E., Davidson,K.K., Lawrence,R.A., Sun,D., Windle,B.E., Hurley,L.H. and Von Hoff,D.D. (1999) Effects of cationic porphyrins as G-quadruplex interactive agents in human tumor cells. *Cancer Res.*, **59**, 639–644.
14. Shin-ya,K., Wierzba,K., Matsuo,K., Ohtani,T., Yamada,Y., Furihata,K., Hayakawa,Y. and Seto,H. (2001) Telomestatin, a novel telomerase inhibitor from Streptomyces anulatus. *J. Am. Chem. Soc.*, **123**, 1262–1263.
15. Burge,S., Parkinson,G.N., Hazel,P., Todd,A.K. and Neidle,S. (2006) Quadruplex DNA: sequence, topology and structure. *Nucleic Acids Res.*, **34**, 5402–5415.
16. Wang,Y. and Patel,D.J. (1993) Solution structure of the human telomeric repeat d[AG3(T2AG3)3] G-tetraplex. *Structure*, **1**, 263–282.
17. Ambrus,A., Chen,D., Dai,J., Bialis,T., Jones,R.A. and Yang,D. (2006) Human telomeric sequence forms a hybrid-type intramolecular G-quadruplex structure with mixed parallel/antiparallel strands in potassium solution. *Nucleic Acids Res.*, **34**, 2723–2735.
18. Luu,K.N., Phan,A.T., Kuryavyi,V., Lacroix,L. and Patel,D.J. (2006) Structure of the human telomere in K+ solution: an intramolecular (3 + 1) G-quadruplex scaffold. *J. Am. Chem. Soc.*, **128**, 9963–9970.
19. Xu,Y., Noguchi,Y. and Sugiyama,H. (2006) The new models of the human telomere d[AGGG(TTAGGG)3] in K+ solution. *Bioorg. Med. Chem.*, **14**, 5584–5591.
20. Phan,A.T., Luu,K.N. and Patel,D.J. (2006) Different loop arrangements of intramolecular human telomeric (3+1) G-quadruplexes in K+ solution. *Nucleic Acids Res.*, **34**, 5715–5719.
21. Dai,J., Punchihewa,C., Ambrus,A., Chen,D., Jones,R.A. and Yang,D. (2007) Structure of the intramolecular human telomeric G-quadruplex in potassium solution: a novel adenine triple formation. *Nucleic Acids Res.*, **35**, 2440–2450.
22. Dai,J., Carver,M., Punchihewa,C., Jones,R.A. and Yang,D. (2007) Structure of the Hybrid-2 type intramolecular human telomeric G-quadruplex in K+ solution: insights into structure polymorphism of the human telomeric sequence. *Nucleic Acids Res.*, **35**, 4927–4940.
23. Phan,A.T., Kuryavyi,V., Luu,K.N. and Patel,D.J. (2007) Structure of two intramolecular G-quadruplexes formed by natural human telomere sequences in K+ solution. *Nucleic Acids Res.*, **35**, 6517–6525.
24. Parkinson,G.N., Lee,M.P. and Neidle,S. (2002) Crystal structure of parallel quadruplexes from human telomeric DNA. *Nature*, **417**, 876–880.
25. He,Y., Neumann,R.D. and Panyutin,I.G. (2004) Intramolecular quadruplex conformation of human telomeric DNA assessed with 125I-radioprobing. *Nucleic Acids Res.*, **32**, 5359–5367.
26. Antonacci,C., Chaires,J.B. and Sheardy,R.D. (2007) Biophysical characterization of the human telomeric (TTAGGG)(4) repeat in a potassium solution. *Biochemistry*, **46**, 4654–4660.
27. Guzman,M.R., Liquier,J., Brahmachari,S.K. and Taillandier,E. (2006) Characterization of parallel and antiparallel G-tetraplex structures by vibrational spectroscopy. *Spectrochimica Acta Part A Mol. Biomol. Spectrosc.*, **64**, 495–503.
28. Juskowiak,B., Galezowska,E., Zawadzka,A., Gluszynska,A. and Takenaka,S. (2006) Fluorescence anisotropy and FRET studies of G-quadruplex formation in presence of different cations. *Spectrochimica Acta Part A Mol. Biomol. Spectrosc.*, **64**, 835–843.
29. Kaushik,M., Bansal,A., Saxena,S. and Kukreti,S. (2007) Possibility of an antiparallel (tetramer) quadruplex exhibited by the double repeat of the human telomere. *Biochemistry*, **46**, 7119–7131.
30. Ourliac-Garnier,I., Elizondo-Riojas,M.A., Redon,S., Farrell,N.P. and Bombard,S. (2005) Cross-links of quadruplex structures from human telomeric DNA by dinuclear platinum complexes show the flexibility of both structures. *Biochemistry*, **44**, 10620–10634.
31. Qi,J.Y. and Shafer,R.H. (2005) Covalent ligation studies on the human telomere quadruplex. *Nucleic Acids Res.*, **33**, 3185–3192.
32. Rujan,I.N., Meleney,J.C. and Bolton,P.H. (2005) Vertebrate telomere repeat DNAs favor external loop propeller quadruplex structures in the presence of high concentrations of potassium. *Nucleic Acids Res.*, **33**, 2022–2031.
33. Paramasivan,S., Rujan,I. and Bolton,P.H. (2007) Circular dichroism of quadruplex DNAs: applications to structure, cation effects and ligand binding. *Methods*, **43**, 324–331.
34. Ying,L., Green,J.J., Li,H., Klenerman,D. and Balasubramanian,S. (2003) Studies on the structure and dynamics of the human telomeric G quadruplex by single-molecule fluorescence resonance energy transfer. *Proc. Natl Acad. Sci. USA*, **100**, 14629–14634.
35. De Cian,A. and Mergny,J.L. (2007) Quadruplex ligands may act as molecular chaperones for tetramolecular quadruplex formation. *Nucleic Acids Res.*, **35**, 2483–2493.
36. Panyutin,I.G. and Neumann,R.D. (1997) Radioprobing of DNA: distribution of DNA breaks produced by decay of 125I incorporated into a triplex-forming oligonucleotide correlates with geometry of the triplex. *Nucleic Acids Res.*, **25**, 883–887.
37. Karamychev,V.N., Zhurkin,V.B., Garges,S., Neumann,R.D. and Panyutin,I.G. (1999) Detecting the DNA kinks in a DNA-CRP complex in solution with iodine-125 radioprobing. *Nat. Struct. Biol.*, **6**, 747–750.
38. Panyutin,I.G. and Neumann,R.D. (1994) Sequence-specific DNA double-strand breaks induced by triplex forming 125I labeled oligonucleotides. *Nucleic Acids Res.*, **22**, 4979–4982.
39. Das,R., Laederach,A., Pearlman,S.M., Herschlag,D. and Altman,R.B. (2005) SAFA: semi-automated footprinting analysis software for high-throughput quantification of nucleic acid footprinting experiments. *RNA*, **11**, 344–354.

40. Marathias,V.M. and Bolton,P.H. (1999) Determinants of DNA quadruplex structural type: sequence and potassium binding. *Biochemistry*, **38**, 4355–4364.
41. Rezler,E.M., Seenisamy,J., Bashyam,S., Kim,M.Y., White,E., Wilson,W.D. and Hurley,L.H. (2005) Telomestatin and diseleno sapphyrin bind selectively to two different forms of the human telomeric G-quadruplex structure. *J. Am. Chem. Soc.*, **127**, 9439–9447.
42. Parkinson,G.N., Ghosh,R. and Neidle,S. (2007) Structural basis for binding of porphyrin to human telomeres. *Biochemistry*, **46**, 2390–2397.
43. Haq,I., Trent,J.O., Chowdhry,B.Z. and Jenkins,T.C. (1999) Intercalative G-Tetraplex Stabilization of Telomeric DNA by a Cationic Porphyrin. *J. Am. Chem. Soc.*, **121**, 1768–1779.
44. Wei,C., Jia,G., Yuan,J., Feng,Z. and Li,C. (2006) A spectroscopic study on the interactions of porphyrin with G-quadruplex DNAs. *Biochemistry*, **45**, 6681–6691.
45. Lubitz,I., Borovok,N. and Kotlyar,A. (2007) Interaction of monomolecular G4-DNA nanowires with TMPyP: evidence for intercalation. *Biochemistry*, **46**, 12925–12929.